Clin Transl Imaging (2013) 1:17–29
DOI 10.1007/s40336-013-0004-4

REVIEW ARTICLE

High-field PET/MRI and MRS: potential clinical and research applications

Valeria Panebianco · Federico Giove · Flavio Barchetti · Franca Podo · Roberto Passariello

Received: 26 November 2012 / Accepted: 17 January 2013 / Published online: 16 February 2013

Abstract Nowadays hybrid PET/MRI systems and magnetic resonance spectroscopy (MRS) with high field strength are becoming more widespread not only in research applications but also in clinical practice. The aim of this paper is to review the current roles of high-field PET/MRI and high-field magnetic resonance spectroscopy (MRS) in the clinical setting and their applications in research. A non-systematic literature search of the Medline and Cochrane Library databases was performed up to September 2012. Bibliographies of retrieved articles and review articles were also examined. Only those articles reporting complete data of clinical and research relevance for the present review (i.e., diagnosis, therapeutic response monitoring) were selected. The advent of higher field strengths (3-T and above), and thus, higher spectral resolution, increased the potentiality and the diffusion of MRS evaluations. This review article is divided into two major parts. The first considers the potential clinical and research roles of MRS at 3-T and of hybrid system PET/MRI, particularly with regard to simultaneous PET/MRI systems which provide some major advantages over the conventional PET/CT systems (such as identical position of the patient during image acquisition, no radiation burden from the MRI part, more structural, functional and molecular imaging at the same time). The second part provides detailed information about the use of ultra-high-field MRS and MRI (7-T) integrated with PET. The fusion of biological information (PET) and morpho-metabolic patterns (MRI–MRS) shows promise for obtaining early diagnosis, coherent follow-up and the desired response to therapy.

Keywords Ultra-high field MRI · High-field MRI · PET/MRI · High-field MRS · Ultra-high field MRS · 3-T MRS

V. Panebianco (✉) · F. Barchetti · R. Passariello
Department of Radiological Sciences, Oncology and Pathology, Sapienza University of Rome, V.le Regina Elena, 324, 00161 Rome, Italy
e-mail: valeria.panebianco@gmail.com

F. Giove
Department of Physics, Sapienza University of Rome, Rome, Italy

F. Podo
Department of Cell Biology and Neurosciences, Istituto Superiore di Sanità, Rome, Italy

Introduction

Ever since the introduction of magnetic resonance imaging (MRI) into clinical practice, the magnitude of the operating magnetic field has shown a slow but steady increase. The inherent increase in signal and spectral information has historically been paralleled by a general development of the scanner hardware and functioning logic, thus, greatly amplifying the information available. Nowadays, the standard fields for clinical and clinical research applications are 1.5 and 3 Tesla (T), respectively; meanwhile an increasing number of higher field (7-T and above) human scale scanners are devoted to the basic research (mainly related to neurosciences), and are now starting to be exploited in clinical research also. On the other hand, positron emission tomography (PET) scanners have evolved comparatively little, with research focusing, rather, on the development of new tracers. Both techniques share a substantial flexibility, deriving from the physical origin of the nuclear magnetic resonance (NMR) signal in one case and from the properties of the tracer in the other. However, MRI enjoys the status of being both a structural and a functional technique, while PET scanners, even the most advanced ones, provide limited

resolution. MRI is capable of imaging anatomy with very high spatial resolution, at organ and tissue level, and with high diagnostic sensitivity. By contrast, PET, using positron-emitting radiopharmaceuticals, furnishes images of functional processes, at cellular and sub-cellular level, with very high diagnostic specificity and high tracer-detection sensitivity (10–11 to 10–12 mol/l). The obvious limitations of PET studies (i.e., low spatial resolution) were initially overcome, albeit partially, by combination with CT, because the building of hybrid PET/CT scanners presented fewer technical problems.

PET/CT scanners, however, suffer from several limitations, including high patient dose and limited soft-tissue contrast, while the combination of PET with MR, by combining the exquisite sensitivity of PET with the versatility of MR, allows the full exploitation of a much wider range of structural and functional information. Among the functional studies, complementary metabolic information can be gathered by PET and magnetic resonance spectroscopy (MRS).

Evidence acquisition

The aim of this paper is to review the current roles of high-field PET/MRI and high-field MRS in the clinical setting and their applications in research. We searched the Medline and Cochrane Library databases in the following fields: ultra-high-field MRI, high-field MRI, PET/MRI, high-field MRS, ultra-high-field MRS, 3-T MRS, 7-T MRS. The search was performed without language restrictions up to September 2012.

High-field (3-T) MRI and MRS

Since their approval by the US Food and Drug Administration, more than a decade ago, there has been a dramatic increase in the installation and use of high-field MR systems operating at 3-T for research purposes and in clinical practice. Offering a substantial increase in signal-to-noise ratio (SNR) compared to standard magnetic field strengths (1.5-T and below), their most important selling point was the achievement of better image quality and the ability to reduce MR data acquisition and overall examination times.

The benefits of 3-T over 1.5-T imaging are seen in those applications with inherently low SNR, such as susceptibility-weighted imaging (SWI), diffusion-weighted imaging (DWI), MR angiography, diffusion tensor imaging (DTI), functional MRI (fMRI), and MRS [1]. However, sometimes, the acquisition times with a 3-T magnet can be even greater than that with a 1.5-T one (i.e., because of prolonged T1 relaxation times) [2].

Switching to a higher field brings several advantages with respect to the well-established MR technique at 1.5-T, namely enhanced spatial and temporal resolutions and also increased sensitivity, thanks to the increased SNR. As far as the MRS is concerned, specific advantages derive from the capability of using smaller voxels or, alternatively, a reduced scanning time, thanks to both the enhanced SNR and the increased spectral resolution. On the other hand, there are also some additional challenges associated with higher field strengths [3], which can be overcome partially with the development of new hardware and software.

The increased spectral resolution provided by a 3-T system compared with a 1.5-T one, for ^{1}H-MRS and ^{31}P-MRS (and other multinuclear applications), allows better discrimination of different metabolite peaks, thus, improving the biochemical tissue characterization. Figure 1 shows an example of the multiplicity of metabolites that can be detected at 3-T, thanks to the achieved increases in SNR and spectral resolution. At this higher field strength, it is also possible to obtain additional metabolic information from healthy tissues [4].

Practically, the superior image quality of 3-T systems as compared with 1.5-T systems has been shown to provide an advantage for neurological, musculoskeletal, and pelvic applications, but this advantage is not so clear for other body applications (neck, thoracic, cardiac and abdominal), mainly due to the still unresolved problem of the high frequency of motion artifacts.

Currently, evidence suggesting an advantage of 3-T systems over 1.5-T systems is good when focusing on technical performance (SNR ratio, image quality, and so on), but relatively low when considering the clinical impact.

Clinical and research applications of MRS at 3-T

The distinction between clinical and research applications of MRS is relatively blurred, due to the fact that no specific reimbursement is provided for MRS for any part of body or disease. Nevertheless, we can separate the two types of application on the basis of standardized utility in clinical practice.

Clinical applications of MRS at 3-T

Hydrogen, the most abundant nucleus in the human body, is also the nucleus most used in clinical MRS applications.

^{1}H-MR spectroscopy at 3-T (3-T ^{1}H-MRS) has been utilized to identify and characterize the metabolic changes associated with many neurological disorders [5]. The list is very long and includes brain tumors (Fig. 2), early diagnosis of degenerative diseases such as Alzheimer's,

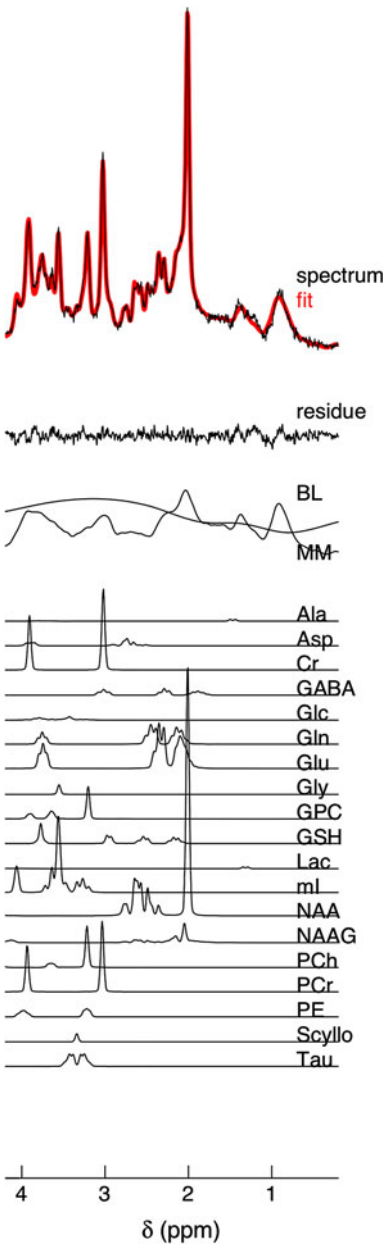

Fig. 1 A ^{1}H MR spectrum acquired at 3-T during a visual paradigm. VOI size 8 ml in the visual cortex, TR/TE 4,000/7 ms, number of transients 60 (acquisition time 4 min). From *top* to *bottom*: RAW spectrum with no post-processing apart from phase correction, LCModel fitting (in *red*), residue of the fitting. Baseline and macromolecular content, fitting of individual metabolites. Spectra like this, acquired with a tailored, high-performance STEAM sequence, contain considerable metabolic information, and allow to reliably quantify 15–20 metabolites. The limited acquisition time allows functional use (i.e., acquisition during different epochs of rest or stimulation), and makes ^{1}H-MRS optimally suited for combination with PET

Huntington's, Parkinson's diseases and amyotrophic lateral sclerosis, cerebrovascular diseases, mild traumatic brain injury, metabolic disorders such as adrenoleukodystrophy and Canavan's disease, and epilepsy. Rare diseases also studied including creatine deficiency syndrome, variant Creutzfeldt–Jakob disease, pantothenate kinase-associated neurodegeneration and Rasmussen's encephalitis.

3-T ^{1}H-MRS also has a broad spectrum of applications outside the neurological field. MRS measures the relative concentrations of certain metabolites within in vivo-selected voxels, such as citrate, creatine, and choline-containing compounds (the so-called total-choline or tCho peak) in the prostate. Citrate levels are reduced in prostate cancer, thus, MRS is a good tool for diagnosing and evaluating aggressiveness of prostate cancer (Fig. 3), monitoring therapy response, and detecting local recurrence after radical prostatectomy [6, 7]. 3-T ^{1}H-MRS has also been used to evaluate treatment (chemotherapy) response in breast cancer. The clinical principle is that increased tCho reflects aberrant metabolism of tumor cells and cell viability, and if the treatment is effective, a decrease in the tCho concentration can be seen even before the occurrence of detectable changes in the tumor's size, vascularity and morphology [8].

MRS at 3-T is also a valid method for detecting the rectal adenocarcinoma and monitoring the treatment response after pre-operative chemoradiotherapy [9].

Furthermore, this approach is an effective, non-invasive technique that can be used to diagnose and quantify hepatic steatosis by detecting the hepatic triglyceride content [10]; it can be an important supplement to the conventional MRI in diagnosing bone and soft-tissue tumors and distinguishing benign from malignant tumors [11] and it opens new research strategies for the early diagnosis of ovarian cancer [12].

Research applications of MRS at 3-T

3-T ^{1}H-MRS has been widely employed in some interesting research fields such as psychiatric diseases (e.g., schizophrenia, depression and bipolar disorders) [13].

With regard to the research in humans, considerable efforts have been directed at evaluating the applicability in MRS of nuclei other than ^{1}H, in particular ^{31}P-MRS.

In cardiac diseases, ^{31}P-MRS is the only non-invasive method for studying the state of myocardial energy metabolism without administering radiopharmaceuticals. This method exploits the signals of the ^{31}P nuclei of high-energy phosphorylated compounds, like phosphocreatine and adenosine triphosphate. On this basis, ^{31}P-MRS can provide an answer to a variety of theoretical and clinical issues in the study of various cardiac diseases, including ischemic heart disease, heart failure and hypertrophic cardiomyopathy of various origins [14].

Recently, 3-T ^{31}P-MRS has been used to evaluate the efficacy of hepatic artery embolization (HAE) in the treatment of neuroendocrine liver metastases. At present, there are no rapid and reliable methods for evaluating the

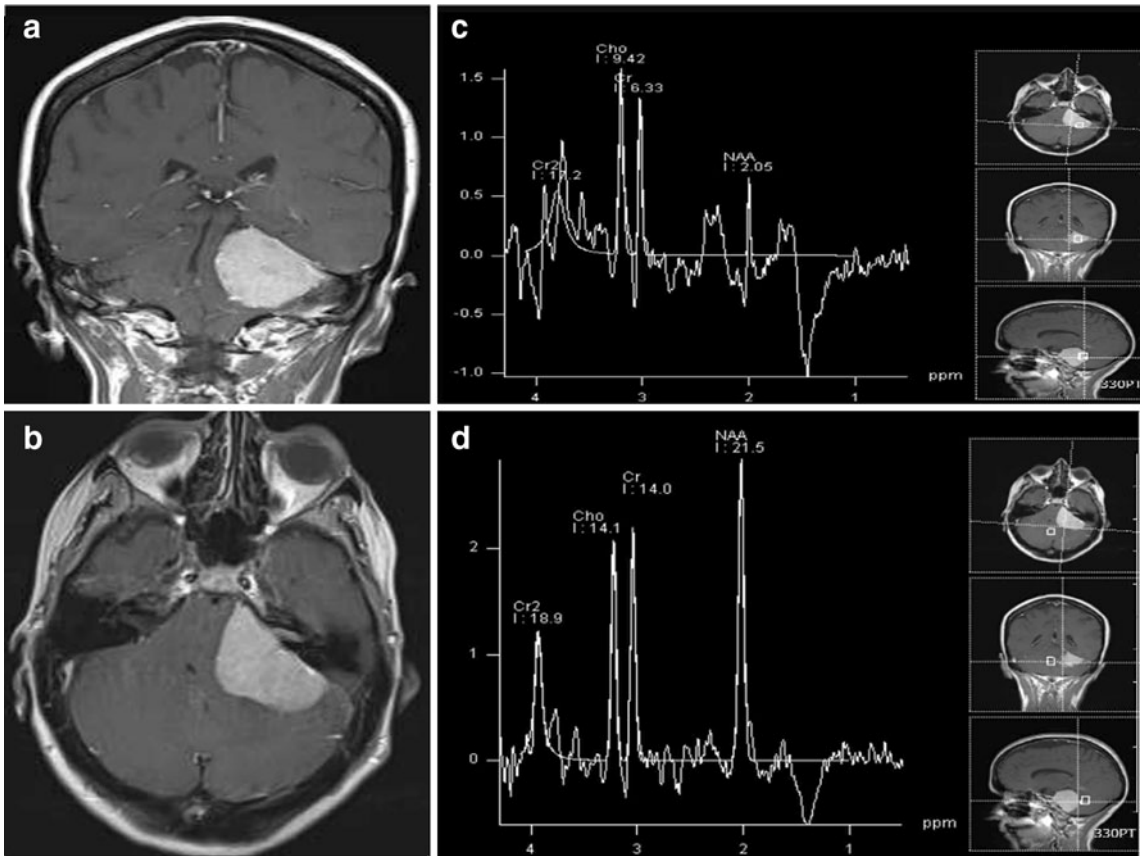

Fig. 2 Courtesy of Prof. P. Pantano, Sapienza University of Rome. A 52-year-old woman with an extraaxial mass at the level of left ponto-cerebellar angle who underwent a 3-T examination. T1-weighted post-gadolinium images in coronal plane (**a**) and axial plane (**b**) showing a lesion with homogeneous enhancement yielding compressive effects on the brainstem, left middle cerebellar peduncle, IV ventricle, left cerebellar hemisphere and slight herniation of the cerebellar tonsils into the foramen magnum. The voxel positioned on the mass (**c**) shows disappearance of the peak of *N*-acetylaspartate (NAA), a small increase in the choline (Cho) peak, appearance of the glutamate/glutamine (Glx) peak and, in particular, appearance of a negative peak at 1.5 ppm; feasible presence of alanine (Ala) which is specific for meningioma. The voxel positioned outside the mass on the normal brain parenchyma (**d**) shows a normal spectrum of the main metabolites

efficacy of HAE in the treatment of neuroendocrine liver metastases. Ljungberg et al. [15] showed significant differences in ^{31}P metabolite ratios between responders and non-responders on the day before HAE, demonstrating the potential of ^{31}P-MRS to predict individual responsiveness prior to HAE.

3-T ^{31}P-MRS has potential in neurological fields also. Examples are the reduction in high-energy phosphates reported in the occipital lobe of migraine without aura patients [16] and new insights provided into the pathobiochemistry of brain damage in multiple sclerosis [17].

3-T ^{31}P-MRS is widely used to measure phosphorus metabolites in muscles, because of its capability to non-invasively monitor the steady-state concentrations of high-energy phosphorus metabolites in resting skeletal muscle and phosphorus metabolite kinetics during exercise and recovery in a single experiment. Therefore, the levels of phosphorus metabolites at rest, and the kinetics of their interconversions during transitions from exercise to rest, have been used to assess muscle energetic status and energy metabolism, both in healthy subjects and in patients with a wide range of diseases [18].

The low sensitivity of ^{13}C-MRS prevents its straightforward use even at 3-T; however, the issue can be partially overcome by the recently developed hyperpolarization techniques [19], by which the magnetization at a given magnetic field can be increased over 10,000-fold above thermal equilibrium. The first applications on humans are ongoing, however, the technique proved very promising on cell cultures and on experimental animal models [20].

MRS could pave the way for the assessment of early tumor responses to therapy and, therefore, prediction of treatment outcome. Using lymphoma-bearing mice injected intravenously with hyperpolarized [1-^{13}C] pyruvate, Day et al. [21] demonstrated that the lactate dehydrogenase (LDH)-catalyzed flux of ^{13}C label between the carboxyl

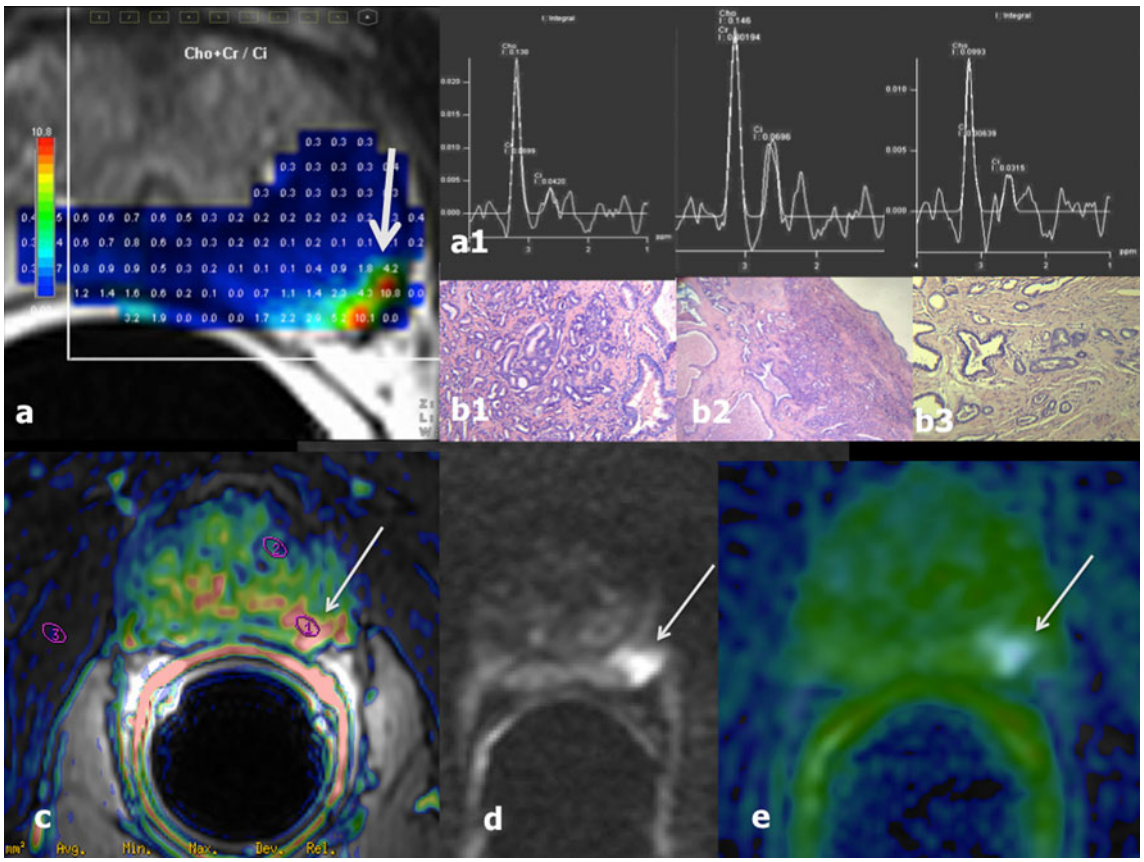

Fig. 3 A 60-year-old patient with a prostate-specific antigen level of 4.2 ng/mL and negative transrectal ultrasound-guided biopsy. **a** Qualitative and quantitative analysis of MRS imaging with reference image on the axial T2-weighted MR (see *arrow* on the posterior left site of the peripheral zone) shows three consecutive voxels (**a1**) with an increased ratio (Cho + Cr/Ci > 1); note the pathological results after radical prostatectomy; GS 7 (3 + 4) in **b1** and **b2** and GS 6 (3 + 3) in **b3**; the other functional techniques also show altered patterns consistent with intermediate–low aggressive prostate cancer: MR perfusion combined with axial T2-weighted image (**c**) and diffusion-weighted image acquired using *b* value 1,000 (**d**) and ADC map (**e**) show neoangiogenesis phenomena and water molecule restriction (see *arrows*), respectively

groups of pyruvate and lactate in the tumor can be measured using ^{13}C-MRS and spectroscopic imaging, and that this flux is inhibited by 24 h after chemotherapy. The reduction in the measured flux after drug treatment and the induction of tumor cell death can be explained by loss of the coenzyme NAD(H) and decreases in the concentrations of LDH and lactate in the tumors.

Witney et al. [22] compared ^{13}C-MRS and spectroscopic-imaging measurements of the uptake and conversion of hyperpolarized [1-^{13}C] pyruvate into [1-^{13}C] lactate in a murine lymphoma model with changes in fluorodeoxyglucose (FDG) uptake after chemotherapy. A decrease in FDG uptake was found to precede the decrease in flux of hyperpolarized ^{13}C label between pyruvate and lactate, both in tumor cells in vitro and in tumors in vivo. However, the magnitude of the decrease in FDG uptake and the decrease in pyruvate to lactate flux was comparable at 24 h after drug treatment. These results show that the measurement of flux between pyruvate and lactate may be used as an adjunct or as an alternative to FDG-PET for imaging the tumor treatment response in the clinic, once ^{13}C hyperpolarization techniques become available at clinical level.

PET/MRI

Simultaneous imaging systems have some major theoretical advantages that could be of interest to the whole medical community. The general advantages of a simultaneous PET/MRI system as compared to a conventional PET/CT system are: (1) recording of dynamic and moving phenomena, which could enable tracers with short half-lives to be studied; (2) identical position of the patient during image acquisition with both modalities leading to a substantial reduction in motion artifacts due to heartbeat, intestinal motion and breathing; (3) absolute match between the tissue information of both modalities under the

same physiological conditions; (4) contrast-enhanced MRI information (e.g., on perfusion and blood flow) can be used in the pharmacokinetic modeling of the PET data, resulting in improved PET reconstruction and data analysis; (5) better localization of the PET signal within the soft tissues; (6) no radiation burden from the MRI part compared with PET/CT, thus, avoiding a radiation dose to the patient of about 25–32 mSv and decreasing the lifetime attributable risk of cancer incidence due to the examination; (7) better application of the one-stop-shop principle for simultaneous diagnostic-quality acquisition of nuclear medicine and radiological images; (8) more structural, functional and molecular imaging at the same time [23, 24].

Clinical applications of PET/MRI and MRS

PET/MRI could offer good potential in the management of diseases in which the MRS has already been shown to play an important role.

Oncology has, by far, been the main clinical area in which the system has been utilized, primarily because of the profile of the institutions that installed the first systems. Thus, prostate (Fig. 4), head/neck, and breast cancers seem to be among the primary indications for PET/MRI [25]. Prostate cancer studies can benefit from PET/MR data fusion. In fact, the heterogeneous features of prostate cancer offer several opportunities for specific PET radiotracers [26], and the information obtained can be merged with metabolic and structural MR data. The proximity with the urinary bladder has a negative impact for tracers that, e.g., FDG, accumulate in that organ. In this case, the development of tailored bimodal TOF PET and MRI probes can help in discriminating the signal from the background noise [27]. In addition, the use of an alternative tracer such as [^{11}C]-choline, characterized by negligible excretion in the urinary tract and low background activity in the pelvis [28], could definitely help in monitoring, in combination with MRS, alterations in choline metabolism associated with cancer progression or therapy response.

Apart from these indications, the system could also be used for lymphoma, melanoma, bone and soft-tissue tumors, gynaecological, hepatic and colorectal malignancies, with the main imaging procedure being whole-body PET/MRI followed by regional MR acquisitions [29, 30]. PET/MRI could also be a powerful tool in identifying liver metastases and in characterizing pancreatic tumors, as demonstrated by previous studies on PET/MRI fusion images which showed high accuracy of this technique, exceeding the performance of PET/CT [31, 32].

Cardiovascular disease is another important clinical area for whole-body PET/MRI. Several centers are currently beginning to incorporate the PET/MRI into cardiovascular imaging, for example, to determine myocardial viability and for the imaging of vulnerable plaques in vessels using FDG; in the future, this approach could be extended to the evaluation of antiangiogenic or stem cell therapies [33]. However, an important limitation of MRI (also at 3-T) emerges in the cardiovascular field, in the evaluation of the distal segments of coronary arteries (which is, instead, possible with coronary CT angiography).

PET/MRI imaging could significantly improve the sensitivity and specificity of the diagnosis and follow-up treatment of infectious and inflammatory diseases. MRI, given the availability of fMRI, DWI, MRS and perfusion imaging, now offers more than just anatomical information. There have also been improvements in MRI contrast agents, which can be used with radiolabeled probes and may lead to even more insights into the dynamics and

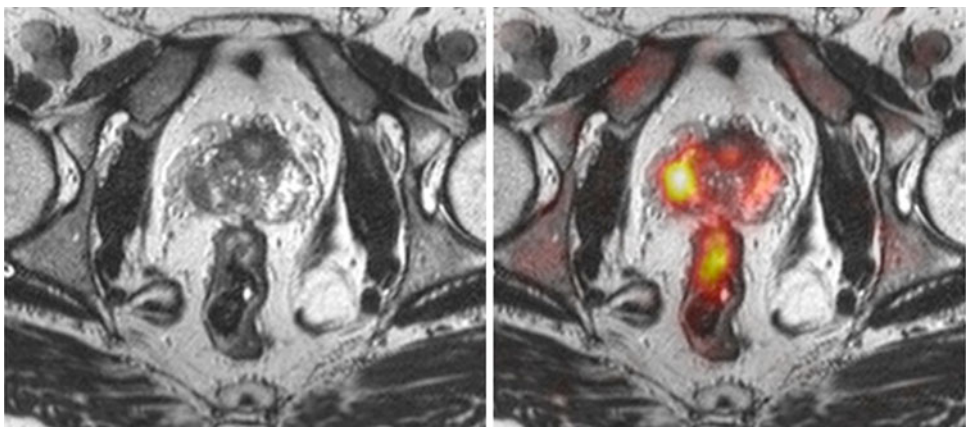

Fig. 4 Courtesy of Prof. Vallée, Prof. Ratib, and Dr Garibotto, Geneva University Hospitals, Ref: Vargas MI, Becker M, Garibotto V, et al. MAGMA 2012 Sep 25. A 58-year-old patient, GS 3 + 3, PSA 5.3 ng/mL. ^{18}F-choline PET/MR images, acquired on the integrated Philips Ingenuity TF PET/MR, combining a 3-T MR tomograph with a time-of-flight PET system. The images show a focal T2 hypointensity in the right peripheral zone, corresponding to an increased ^{18}F-fluorocholine uptake

characteristics of the inflammatory process. MRI-based motion correction is a third interesting feature of PET/MRI, given that it would allow more accurate quantification of PET data, leading to better treatment monitoring and the possibility of earlier response evaluation.

PET/MRI could detect epileptogenic areas in patients with tuberous sclerosis complex, who are potential surgical candidates if the epileptogenic regions can be accurately identified [34].

PET/MRI may be also very useful in patients with cortical dysplasia who are difficult to treat, because the MRI abnormality may be undetectable [35].

Research applications of PET/MRI and MRS

Multiple research efforts are today devoted to identifying the conditions in which the advantages offered by PET/MR integration can go far beyond the simple acquisition of functional PET information under structural MRI guidance. In this context, it has been proposed that the combination of anatomical MRI, DWI and PET imaging, to obtain concerted information about the cellularity and biological activity of a tumor (i.e., by the use of FDG, ^{18}F-fluorodeoxythymidine, or radiolabeled choline), may indeed result in enhanced accuracy in staging, as well as in assessing tumor spread to lymph nodes, especially not only in the pelvis but also in the mediastinum and head and neck region [36].

Another area in which a combination of multiple functional imaging approaches such as PET and MR could be particularly valuable is the non-invasive identification and monitoring of novel biomarkers of tumor response to targeted therapies. Investigations for the detection of conventional markers are, in fact, often costly and time consuming and may even require repeated tissue biopsies to overcome the problems deriving from tumor heterogeneity, differences from primary tumor to metastases, and modifications induced by changes in the tumor microenvironment. By allowing simultaneous, non-invasive and longitudinal examinations of both the primary tumor and its metastases, multimodality molecular-imaging protocols are, therefore, expected to impact greatly on the progress of personalized medicine [36].

MRS and PET can both be used to monitor metabolic processes and products in vivo. However, one has to bear in mind that these methods may differ not only in sensitivity and spatial resolution [37] but also, substantially, in the specific sets of molecular events and enzymatic reactions examined within a given metabolic pathway. The latter aspect can actually represent a crucial advantage of an integrated PET/MRS approach. The different information on glycolysis that can be provided by the two methods is a case in point.

Monitoring glucose metabolism yields precious information about energetic processes in vivo. FDG is the most widely used PET tracer and is routinely applied to measure the glucose consumption in cardiology, neurology and oncology. Unlike glucose, FDG cannot proceed down the glycolysis pathway and thus remains trapped, as FDG-6-phosphate, in the tissue. Therefore, FDG-PET gives essential information about glucose transport and hexokinase activity at the first reaction step of the glycolytic reaction cascade.

On the other hand, MRS methods (especially those based on ^{13}C hyperpolarization) are able to image the changes in the relative flux rates of pyruvate, the end product of the glycolytic reaction cascade, in the different reactions, respectively, responsible for its conversion into acetyl-CoA (to fuel the tricarboxylic cycle), lactate or alanine. The different "biochemical windows" explored by FDG-PET and MRS in tumors are schematically represented in Fig. 5. The complementarity of information provided by these molecular-imaging procedures resides in the fact that they measure different effects of the same phenomenon by which the mitochondrial ATP is redirected to glucose phosphorylation in cancer cells. This "bioenergetic switch", closely related to Otto Warburg's [38] discovery of enhanced glycolysis of tumor cells under normoxic conditions, is today classified as a cancer hallmark and is held responsible for the capability of cancer cells to maintain a high proliferative rate under conditions of oncogene-driven cell signaling activation. For these reasons, the standardized uptake value of FDG-PET and MRS profiles may actually serve as biomarkers of tumor progression and/or response to anticancer agents. The comparison and combination of PET/MR information are, therefore, of special interest for tumor treatment studies, as they reveal that which part of the glucose metabolism pathway is targeted by an anticancer agent [39] or by a targeted therapy (e.g., imatinib mesylate [40]).

The different roles of PET and MRS in measuring metabolic fluxes in the aberrant phosphatidylcholine (PtdCho) cycle in cancer cells provide another example of the complementarity of the biochemical information furnished by these molecular-imaging modalities in cancer tissues.

In fact, while choline-based PET essentially measures choline transport and phosphorylation in the Kennedy pathway, the profile of the ^{1}H-MRS-detected tCho peak (mainly comprising contributions from phosphocholine, glycerophosphocholine and free choline) reflects the activities of the multiple enzymes involved in both biosynthetic and catabolic pathways of the PtdCho cycle [41].

Furthermore, PET and MRS are providing unique information on drug biodistribution, targeting, metabolism and pharmacokinetics/pharmacodynamics (PK/PD). PET using drugs radiolabeled with ^{11}C and ^{18}F is the technique

of choice for PK/PD studies, whereas the nuclei most suitable for PK/PD studies using MRS are ^{1}H, ^{13}C, ^{19}F and ^{31}P. The development of a single combined hybrid PET/MRI instrument able to perform PET and MRI/MRS measurements simultaneously can allow a better study of drug kinetics [42].

Ultra-high-field (7-T) MRI and MRS

Since the first 7 and 8-T human scale scanners were installed in the late 1990s, an increasing number of research centers have adopted the ultra-high-field (UHF, 7-T and above) NMR technology for human studies. Currently, 7-T whole-body and head scanners are available or planned in more than 50 sites around the world, and are being installed at a rate of about 1/month. Significant efforts have been made to solve the technical problems related to UHF NMR [43] and some of these developments have filtered down to lower-field applications. As a consequence, UHF scanners are currently being installed in hospitals also, even though body imaging is still not ready for general utilization, and mature clinical applications are restricted to neuroradiology.

The main advantages of UHF technology include higher SNR and spectral dispersion, which imply potentially higher spatial, temporal, and spectral resolution. These are the features equally useful in research and in clinical practice. Besides these general advantages, some specific techniques, which exploit susceptibility effects, enjoy the specific benefit of increased sensitivity, because the phenomenon itself is enhanced. These techniques include functional fMRI and SWI.

Research applications (7-T)

As well as in a huge amount of technologically oriented work, the advantages of high fields also emerged, from the very beginning, in functional studies. UHF fMRI has been shown to be capable of detecting brain functional changes at columnar and laminar levels in the visual cortex [44], thanks to the increased spatial resolution and specificity that UHF technology allows. Combination with electrophysiological techniques allowed satisfactory insights into neurovascular coupling [45]. In a similar fashion, functional MRS has been exploited to follow the metabolic changes induced by stimulation [46]. Although possible, imaging and spectroscopy with low gyromagnetic ratio nuclei at UHF has seldom been exploited in man (the main applications include ^{13}C, ^{31}P, ^{17}O and ^{23}Na imaging and/or spectroscopy). On the other hand, its use in animals is much more developed, and in fact, several important studies on metabolism and energetics have been published, mainly based on ^{13}C and ^{31}P spectroscopy [47–49].

Until recent years, morphological imaging at UHF was hampered by specific absorption ratio (SAR) and technical issues, especially in the body. A UHF has the potential to increase the imaging resolution well above the values that are practical at 3-T, and the shorter wavelength of the B_1 field, while a problem in itself, allows a high degree of

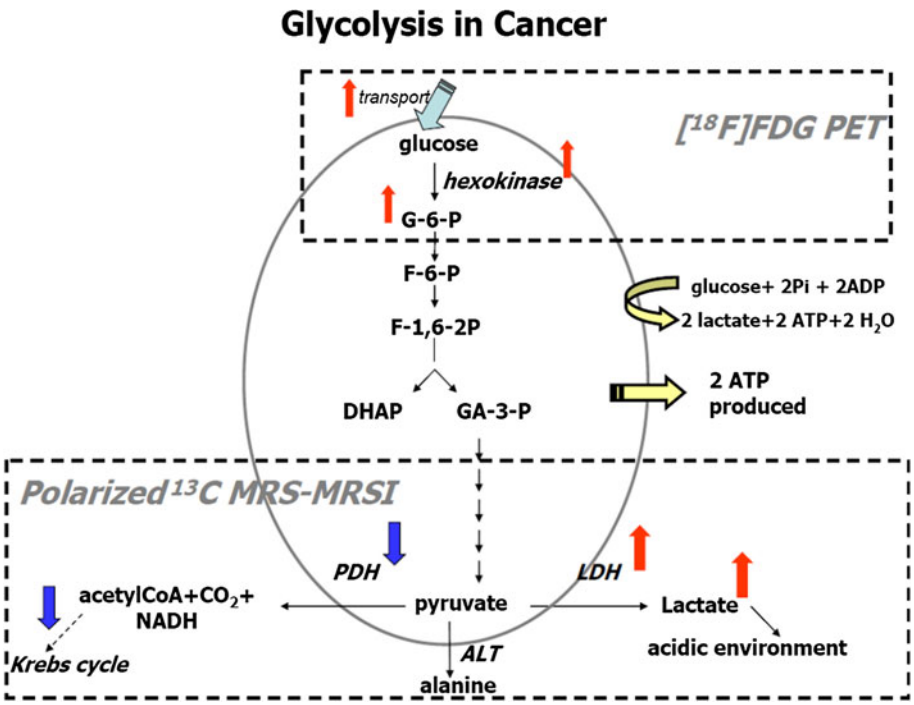

Fig. 5 Molecular bases of metabolic imaging of glycolysis in cancer. Metabolites: *DHAP* dihydroxyacetone phosphate, *G-6-P* glucose 6-phosphate, *GA-3-P* glyceraldehydes 3-phosphate, *F-1,6-2P* fructose 1,6-bisphosphate, *F-6-P* fructose 6-phosphate. Enzymes: *ALT* aminotransferase, *LDH* lactate dehydrogenase, *PDH* pyruvate dehydrogenase. Methods: *PET* positron emission tomography, *MRS* magnetic resonance spectroscopy, *MRSI* magnetic resonance spectroscopic imaging. Tracer: *[^{18}F]FDG* [(18)F]fluoro-2-deoxy-D-glucose

parallel imaging. The latter is able to mitigate some of the B_0 dishomogeneity problems by reducing the time needed for the readout train [50], while during transmission, it is expected to help keep SAR under control and/or increase excitation uniformity via B_1 shimming [51]. Thus, much of the research has focused on technical issues. However, conventional as well as advanced structural imaging techniques are increasingly being exploited in clinical neurology research [52, 53].

Clinical applications (7-T)

Clinical applications of UHF MR include, mainly, neuroradiological applications.

Most clinical reports and potential clinical applications of 7-T are, at present, found in the field of multiple sclerosis where a 7-T magnet allows increased lesion detection in cortical gray matter compared with a 3-T magnet [54].

One of the most widely envisaged applications is the pre-operative mapping of lesions and/or functionally eloquent areas by fMRI, SWI, DTI or anatomical imaging. This approach is currently applied, at lower fields, in pathologies that range from epilepsy to cancer and cortical dysplasia; the switch to UHF can offer better resolution and specificity, especially in fMRI and SWI. UHF SWI itself was shown to be sensitive to tissue iron content [55], with possible applications in neurodegenerative diseases and vascular imaging. It has been shown that, in spite of SAR limitations, all the clinical information available at 3-T in subacute and chronic stroke patients is present also at 7-T; beyond that, UHF imaging offers more anatomical detail [56]. In clinical settings, anatomical high-resolution MR has also been proven to be useful in neurodegenerative diseases [57] and in brain tumor management [58]. Other UHF clinical applications include angiography [59], cardiac and cardiovascular imaging [60], musculoskeletal imaging [61], renal imaging [62], and breast imaging [63].

Integration with PET

UHF MR applications fully exploit the fact that the NMR signal is intrinsically multiparametric, and can be made sensitive to several biophysical phenomena, related to either tissue structure or function. Indeed, the MR techniques can be roughly divided into two categories: static and dynamic approaches. Static approaches (like all the structural techniques) measure tissue properties that are stationary, or change with time scales that are much longer than the integrated measurement time. Dynamic approaches are made sensitive to the change of the system during the measurement itself, and indeed tend to measure differences that are externally triggered. All functional approaches (fMRI, fMRS) belong to this group. The time scale during which the system evolution is observable (i.e., the temporal resolution) is inferiorly limited by the measurement repetition time (magnitude order of 1 s), while the total duration can extend to as much as several tenths of a minute.

In the context of PET/MR combination, the first aim is to fuse the intrinsic functional information of the PET scan with the detailed anatomical, thus static, information provided by the MR modality. Post-processing fusion of data obtained from distinct single-modality scanners is feasible but suboptimal because of the poor anatomical detail of the PET scans that does not allow satisfactory co-registration. Even though interim solutions with tandem scanners served by a single-rail guided patient bed are feasible [64], the optimal solution is clearly the integration of the two modalities in a single scanner, as has been done for PET/CT. The availability of a commercial 3-T PET/MR scanner showed that it is feasible at human scale, even though higher-field combined scanners are currently available only for animal studies. The advantages of PET/MRI versus PET/CT combined scanners include superior MR performances in soft-tissue contrast and reduced radiation dose of the combined study (a feature especially appreciated in cancer follow-up), but the main envisaged improvement is the possibility of fully exploiting all the MR modalities, including dynamic data, that contribute functional information potentially complementary to the PET data. In this context, the possibility of acquiring PET and MR data simultaneously (as opposed to sequentially, as done with PET/CT) is a key feature (although actually commercial PET/MR integrated modalities are also offered as sequential devices). Indeed, this approach not only reduces the total scan time but also allows direct comparison of dynamic changes (or steady states) induced by the same challenge (i.e., a pharmacological challenge, or a stimulation). While these basic advantages are intrinsic to 3-T PET/MR also, in this section, we will discuss issues relating specifically to UHF MR in combination with PET. In particular, dynamic studies are expected to benefit from UHF MR/PET integration, while conventional structural MR studies acquired for anatomical reference of the PET data can be more straightforwardly performed on 3-T MR/PET scanners.

UHF PET/MR systems are currently not available as commercial systems; however, some viable solutions have been studied and implemented in several prototypes. From a technical point of view, the same schemes developed for lower fields can work at UHF. In particular, the PET readout electronics can be based on photomultipliers, which are magnetic field sensitive devices, and thus, must be located at a magnetic field-shielded area far from the scanner. As a consequence, the unamplified scintillation

light must be routed to the photomultipliers via optical fibers, a solution that allows minimal interference of PET with MR, but significantly degrades PET signal energy and temporal resolution. An alternative solution is to base the PET readout on solid-state devices (avalanche photodiodes or silicon photomultipliers) that can be directly coupled to the scintillator. Similar solutions have been shown to work at 7-T [65] and at 9.4-T [66], and are better described in other papers in this issue.

Intermodal validation and information fusion

While, in principle, both PET and MR can perform quantitative measurements of physiological parameters, quantitation relies on a number of assumptions and calibrations. A typical example is the brain perfusion measurement (CBF), a parameter of great clinical and scientific interest, which can be measured non-invasively by MRI via arterial spin labeling (ASL), or using an appropriate contrast agent with MR (paramagnetic contrast agents) or with PET (usually $H_2^{15}O$). Simultaneous measurement with PET and MRI would allow better calibration of the techniques and clarification of the relevant limitations. This is especially true with ASL at high field, where the related physiological issues are further complicated by the comparably low uniformity of the RF field, which makes blood water labeling less controllable. A better understanding of the blood oxygenation level dependent (BOLD) effect can also be expected, for instance, through better assessment of the spatial distribution of the signal (intravascular or tissue, in proximity of small or large vessels), and a more detailed characterization of the interplay between metabolic and vascular parameters, which generates the dynamic features of the BOLD signal. In this context, a PET-based exploration of the limitations and features of the so-called calibrated BOLD approach for cerebral metabolic rate of oxygen ($CMRO_2$) measurement [67] would be important. Combined and reliable metabolic and functional measurements are, of course, crucial in the study of brain energetics, as well as in the assessment of neurophysiological and neurometabolic coupling [68]. Interestingly, PET kinetic modeling also can be improved by simultaneous MR-derived measurements, including CBF [69].

A straightforward application of combined PET/MR in dynamic studies would be the combination of FDG-PET with ^{1}H-, ^{13}C- and ^{31}P-MRS. FDG-PET can, in fact, provide information about the rate of glycolysis, while MRS can simultaneously monitor the rate of the tricarboxylic acid cycle and the tissue energy status. In this context, ^{1}H-MRS has the clear disadvantage of providing poorer information compared to ^{13}C-MRS. However, high-field ^{1}H-MRS has been successfully exploited for the characterization of brain energetics in humans [70], because the high sensitivity of proton MRS easily allows dynamic studies. The low gyromagnetic ratio of ^{13}C, as well as the problems related to the need for appropriate isotopic enrichment, do not prevent functional studies on carbon compounds, even though these require long scan times [71]. The combined functional acquisition of FDG-PET and MRS data can be helpful not only in the study of brain physiology but also in the characterization of tumor metabolism, and ultimately in cancer diagnostics.

A second dynamic application would be the multiparametric study of brain function. While MR is in principle capable of performing simultaneous measurement of BOLD, CBF, and also cerebral blood volume (CBV) and (indirectly) $CMRO_2$, the PET modality would make it possible to independently monitor one parameter (CBF, for instance) to reduce the impact of signal modeling, or to add further information by means of cerebral metabolic rate of glucose consumption assessment via FDG. Depending on the tracer, the average acquisition time of PET can exceed the fMRI acquisition time by an order of magnitude or even more, thus, preventing direct correlation of results. However, approaches for combined analysis can be developed, as has been done, for instance, for simultaneous EEG/fMRI acquisitions.

A more basic potential advantage is the possibility of applying motion correction to PET functional data acquired simultaneously to fMRI EPI series, allowing an increase of the spatial specificity of PET data up to their nominal spatial resolution [72]. A similar advantage of PET data can arise from tailored partial volume correction, based on the excellent MRI discrimination of soft tissues and high spatial resolution [73]. This can be especially useful in small or heterogeneous structures, like tumors.

Studies on stroke, cardiac ischemia, and on cancer progression and treatment will benefit from PET/MR approaches, thanks to the combination of information about tissue perfusion, metabolic changes (lactate, *N*-acetylaspartate), microscopic damage (DWI), and degree of tissue hypoxia (^{18}F-fluoromisonidazole, and other PET tracers). A related issue is the characterization of angiogenesis, especially in tumors, and the assessment of therapeutic antiangiogenic treatments. The combined use of dynamic contrast-enhanced MRI for the assessment of vascular permeability, and of PET angiogenesis markers could probably be complemented by other MR techniques sensitive to microperfusion, like intravoxel incoherent motion measurements.

The specific role of UHF MR and PET combination will be related essentially to the higher attainable spatial resolution. In conjunction with tailored contrast agents, such as micro- and nanoparticles, UHF MR imaging has been shown to be able to detect in vivo in rats single-labeled cells [74]. This ability can be combined with PET

assessment of cell function or metabolism in many fields, including tracking of implanted stem cells [75, 76]. Interestingly, dual mode functionalized PET/MR nanoprobes have been developed, and can be exploited, in principle, for spatially tracking (via MR) the nanoparticle, while the radiolabeled payload would allow quantitation of the uptaken/interacting biomarker [77]. Future developments may include intelligent probes and drug delivery.

Final considerations

Hybrid PET/MRI systems and MRS with high field strength are becoming more widespread not only in research applications but also in clinical settings. Combining morpho-metabolic (MRI–MRS) and functional information (PET), using a high-performance magnet (3, 7-T), is the most reliable way of obtaining increased sensitivity in cancer detection and assessment of aggressiveness. In fact, optimal spectral resolution (heteronuclear MRS) combined with high contrast resolution (MRI) can, in association with functional PET information, dramatically improve the early diagnosis. In addition, nowadays MRI, thanks to functional fMRI, DWI, MRS and perfusion imaging, offers more than just anatomical information. The fields of application are numerous: brain tumors, early diagnosis of degenerative diseases and other neurological and psychiatric disorders (i.e., Alzheimer, schizophrenia), oncology (prostate, breast, gynecological cancers), cardiovascular and inflammatory diseases. Further studies and with larger patient populations are needed to confirm the clinical relevance of these combined methods.

Conflict of interest None.

References

1. Wattjes MP, Barkhof F (2012) Diagnostic relevance of high field MRI in clinical neuroradiology: the advantages of driving a sport car. Eur Radiol 22(11):2304–2306. doi:10.1007/s00330-012-2552-9
2. Zapparoli M, Semelka RC, Altun E et al (2008) 3.0-T MRI evaluation of patients with chronic liver diseases: initial observations. Magn Reson Imaging 26(5):650–660. doi:10.1016/j.mri.2008.01.037
3. Van der Graaf M (2010) In vivo magnetic resonance spectroscopy: basic methodology and clinical applications Eur Biophys J 39(4):527–540
4. Shukla-Dave A, Hricak H, Moskowitz C, Ishill N, Akin O, Kuroiwa K, Spector J, Kumar M, Reuter VE, Koutcher JA, Zakian KL (2007) Detection of prostate cancer with MR spectroscopy imaging: an expanded paradigm incorporating polyamines. Radiology 245(2):499–506
5. Di Constanzo A, Trosji F, Tosetti M et al (2007) Proton MR spectroscopy of the brain. An update. Eur Radiol 17:1651–1662
6. Kobus T, Vos PC, Hambrock T et al (2012) Prostate cancer aggressiveness: in vivo assessment of MR spectroscopy and diffusion-weighted imaging at 3 T. Radiology 265(2):457–467. doi:10.1148/radiol.12111744
7. Panebianco V, Sciarra A, Lisi D et al (2012) Prostate cancer: ^{1}HMRS-DCEMR at 3T versus [(18)F]choline PET/CT in the detection of local prostate cancer recurrence in men with biochemical progression after radical retropubic prostatectomy (RRP). Eur J Radiol 81(4):700–708
8. Nelson MT, Everson LI, Garwood M, Emory T, Bolan PJ (2008) MR spectroscopy in the diagnosis and treatment of breast cancer. Semin Breast Dis 11(2):100–105
9. Kim MJ, Lee Sj, Lee JH et al (2012) Detection of rectal cancer and response to concurrent chemoradiotherapy by proton magnetic resonance spectroscopy. Magn Reson Imaging 30(6):848–853
10. Georgoff P, Thomasson D, Louie A et al (2012) Hydrogen-1 MR spectroscopy for measurement and diagnosis of hepatic steatosis. Am J Roentgenol 199(1):2–7
11. Fayad LM, Wang X, salibi N et al (2010) A feasibility study of quantitative molecular characterization of musculoskeletal lesions by proton spectroscopy at 3 T. Am J Roentgenol 195(1):W69–W75
12. McLean MA, Priest AN, Joubert I et al (2009) Metabolic characterization of primary and metastatic ovarian cancer by ^{1}H-MRS in vivo at 3T. Magn Reson Med 62(4):855–861
13. Tayoshi S, Sumitani S, Taniguchi K et al (2009) Metabolite changes and gender differences in schizophrenia using 3-Tesla proton magnetic resonance spectroscopy (^{1}H-MRS). Schizophr Res 108(1-3):69–77
14. El-Sharkawy AM, Schär M, Ouwerkerk R, Weiss RG, Bottomley PA (2009) Quantitative cardiac ^{31}P spectroscopy at 3 T using adiabatic pulses. Magn Reson Med 61(4):785–795
15. Ljungberg M, Westberg G, Vikhoff-Baaz B et al (2012) ^{31}P MR spectroscopy to evaluate the efficacy of hepatic artery embolization in the treatment of neuroendocrine liver metastases. Acta Radiol 53(10):1118–1126. doi:10.1258/ar.2012.120050
16. Reyngoudt H, Paemeleire K, Descamps B (2011) ^{31}P-MRS demonstrates a reduction in high-energy phosphates in the occipital lobe of migraine without aura patients. Cephalagia 31(12):1243–1253
17. Hattingen E, Magerkurth J, Pilatus U et al (2011) Combined (1)H and (31)P spectroscopy provides new insights into the pathobiochemistry of brain damage in multiple sclerosis. NMR Biomed 24(5):536–546. doi:10.1002/nbm.1621
18. Edwards LM, Tyler DJ, Kemp GJ et al (2012) The reproducibility of 31-phosphorus MRS measures of muscle energetics at 3 Tesla in trained men. PLoS One 7(6):e37237. doi:10.1371/journal.pone.0037237.Epub2012Jun11
19. Gallagher FA, Kettunen MI, Brindle KM (2009) Biomedical applications of hyperpolarized ^{13}C magnetic resonance imaging. Prog Nucl Magn Reson Spectrosc 55:285–295
20. Kurhanewicz J, Vigneron DB, Brindle K et al (2011) Analysis of cancer metabolism by imaging hyperpolarized nuclei: prospects for translational to clinical research. Neoplasia 13(2):81–97
21. Day SE, Kettunen MI, Cherukuri MK, Mitchell JB, Lizak MJ, Morris HD, Matsumoto S, Koretsky AP, Brindle KM (2011) Detecting response of rat C6 glioma tumors to radiotherapy using hyperpolarized [1-^{13}C]pyruvate and ^{13}C magnetic resonance spectroscopic imaging. Magn Reson Med 65(2):557–563. doi:10.1002/mrm.22698.Epub2010Nov16
22. Witney TH, Kettunen MI, Day SE, Hu DE, Neves AA, Gallagher FA, Fulton SM, Brindle KM (2009) A comparison between radiolabeled fluorodeoxyglucose uptake and hyperpolarized (13)C-labeled pyruvate utilization as methods for detecting tumor response to treatment. Neoplasia 11(6):574–582 (1 p following 582)

23. Glaudemans AW, Quitero AM, Signore A (2012) PET/MRI in infectious and inflammatory diseases: will it be a useful improvement? Eur J Nucl Med Mol Imaging 39(5):745–749
24. Huang B, Law MW, Khong PL (2009) Whole-body PET/CT scanning: estimation of radiation dose and cancer risk. Radiology 251(1):166–174. doi:10.1148/radiol.2511081300
25. Buchbender C, Heusner TA, Lauenstein TC et al (2012) Oncologic PET/MRI, part 1: tumors of the brain, head and neck, chest, abdomen, and pelvis. J Nucl Med 53(6):928–938
26. Castellucci P, Jadvar H (2012) PET/CT in prostate cancer: non-choline radiopharmaceuticals. Q J Nucl Med Mol Imaging 56:367–374
27. Garibaldi F, Capuani S, Colillia S et al (2012) TOPEM: A PET-TOF endorectal probe, compatible with MRI for diagnosis and follow up of prostate cancer. Nucl Instrum Methods Phys Res A 702:13–15. doi:10.1016/j.nima2012.09.020
28. Kobori O, Kirihara Y, Kosaka N, Hara T (1999) Positron emission tomography of esophageal carcinoma using (11)C-choline and (18)F-fluorodeoxyglucose: a novel method of preoperative lymph node staging. Cancer 86(9):1638–1648
29. Nakajo K, Tatsumi M, Inoue A et al (2010) Diagnostic performance of fluorodeoxyglucose positron emission tomography/magnetic resonance imaging fusion images of gynecological malignant tumors: comparison with positron emission tomography/computed tomography. Jpn J Radiol 28(2):95–100
30. Buchbender C, Heusner TA, Lauenstein TC et al (2012) Oncologic PET/MRI, part 1: tumors of the brain, head and neck, chest, abdomen, and pelvis. J Nucl Med 53(8):1244–1252. doi:10.2967/jnumed.112.109306
31. Yong TW, Yuan ZZ, Jun Z et al (2011) Sensitivity of PET/MR images in liver metastases from colorectal carcinoma. Hell J Nucl Med 14(3):264–268
32. Tastumi M, Isohashi K, Onishi H et al (2001) ^{18}F-FDG PET/MRI fusion in characterising pancreatic tumors: comparison to PET/CT. Int J Clin Oncol 16(4):408–415
33. Nekolla SG, Martinez-Moeller A, Saraste A (2009) PET and MRI in cardiac imaging: from validation studies to integrated applications. Eur J Nucl Med Mol Imaging 36(Suppl 1):S121–S130
34. Chandra PS, Salamon N, Huang J et al (2006) FDG-PET/MRI coregistration and diffusion-tensor imaging distinguish epileptogenic tubers and cortex inpatients with tuberous sclerosis complex: a preliminary report. Epilepsia 47(9):1543–1549
35. Salamon N, Kung J, Shaw SJ et al (2008) FDG PET/MRI coregistration improves detection of cortical dysplasia in patients with epilepsy. Neurology 71(20):1594–1601
36. Balyasnikova S, Löfgren J, de Nijs R et al (2012) PET/MR in oncology: an introduction with focus on MR and future perspectives for hybrid imaging. Am J Nucl Med Mol Imaging 2(4):458–474
37. Bohndiek SE, Brindle KM (2010) Imaging and "omic" methods for the molecular diagnosis of cancer. Expert Rev Mol Diagn 10(4):417–434
38. Warburg O (1956) On the origin of cancer cells. Science 123(3191):309–314
39. Wehrl HF, Judenhofer, Wiehr S et al (2009) Pre-clinical PET/MR: technological advances and new perspectives in biomedical research. Eur J Nucl Med Mol Imaging 36(Suppl 1):S56–S68
40. Serkova N, Boros LG (2005) Detection of resistance to imatinib by metabolic profiling: clinical and drug development implications. Am J Pharmacogenomics 5(5):293–302
41. Podo F, Canevari S, Canese R et al (2011) MR evaluation of response to targeted treatment in cancer cells. NMR Biomed 24(6):648–672
42. Wolf W (2011) The unique potential for noninvasive imaging in modernizing drug development and in transforming therapeutics: PET/MRI/MRS Pharm Res 28(3):490–493
43. Moser E, Stahlberg F, Ladd ME, Trattnig S (2012) 7-T MR—from research to clinical applications? NMR Biomed 25:695–716. doi:10.1002/nbm.1794
44. Yacoub E, Shmuel A, Logothetis N, Ugurbil K (2007) Robust detection of ocular dominance columns in humans using Hahn Spin Echo BOLD functional MRI at 7 Tesla. Neuroimage 37:1161–1177. doi:10.1016/j.neuroimage.2007.05.020
45. Logothetis NK (2008) What we can do and what we cannot do with fMRI. Nature 453:869–878. doi:10.1038/nature06976
46. Mangia S, Tkac I, Gruetter R, Van de Moortele PF, Maraviglia B, Ugurbil K (2007) Sustained neuronal activation raises oxidative metabolism to a new steady-state level: evidence from ^{1}H NMR spectroscopy in the human visual cortex. J Cereb Blood Flow Metab 27:1055–1063. doi:10.1038/sj.jcbfm.9600401
47. Rothman DL, De Feyter HM, de Graaf RA, Mason GF, Behar KL (2011) ^{13}C MRS studies of neuroenergetics and neurotransmitter cycling in humans. NMR Biomed 24:943–957. doi:10.1002/nbm.1772
48. Zhu XH, Du F, Zhang N, Zhang Y, Lei H, Zhang X, Qiao H, Ugurbil K, Chen W (2009) Advanced in vivo heteronuclear MRS approaches for studying brain bioenergetics driven by mitochondria. Methods Mol Biol 489:317–357. doi:10.1007/978-1-59745-543-5_15
49. Zhu XH, Zhang N, Zhang Y, Zhang X, Ugurbil K, Chen W (2005) In vivo ^{17}O NMR approaches for brain study at high field. NMR Biomed 18:83–103. doi:10.1002/nbm.930
50. Wiesinger F, Van de Moortele PF, Adriany G, De Zanche N, Ugurbil K, Pruessmann KP (2006) Potential and feasibility of parallel MRI at high field. NMR Biomed 19:368–378. doi:10.1002/nbm.1050
51. Setsompop K, Alagappan V, Zelinski AC, Potthast A, Fontius U, Hebrank F, Schmitt F, Wald LL, Adalsteinsson E (2008) High-flip-angle slice-selective parallel RF transmission with 8 channels at 7 T. J Magn Reson 195:76–84. doi:10.1016/j.jmr.2008.08.012
52. Versluis MJ, van der Grond J, van Buchem MA, van Zijl P and Webb AG (2012) High-field imaging of neurodegenerative diseases. Neuroimaging Clin N Am 22:159–171, ix. doi:10.1016/j.nic.2012.02.005
53. Metcalf M, Xu D, Okuda DT, Carvajal L, Srinivasan R, Kelley DA, Mukherjee P, Nelson SJ, Vigneron DB, Pelletier D (2010) High-resolution phased-array MRI of the human brain at 7 tesla: initial experience in multiple sclerosis patients. J Neuroimaging 20:141–147. doi:10.1111/j.1552-6569.2008.00338.x
54. De Graaf WL, Kilsdonk ID, Lopez-Soriano A, Zwanenburg JJ, Visser F, Polman CH, Castelijns JA, Geurts JJ, Pouwels PJ, Luijten PR, Barkhof F, Wattjes MP (2013) Clinical application of multi-contrast 7-T MR imaging in multiple sclerosis: increased lesion detection compared to 3 T confined to grey matter. Eur Radiol 23(2):528–540. doi:10.1007/s00330-012-2619-7
55. Yao B, Li TQ, Gelderen P, Shmueli K, de Zwart JA, Duyn JH (2009) Susceptibility contrast in high field MRI of human brain as a function of tissue iron content. Neuroimage 44:1259–1266. doi:10.1016/j.neuroimage.2008.10.029
56. Madai VI, von Samson-Himmelstjerna FC, Bauer M, Stengl KL, Mutke MA, Tovar-Martinez E, Wuerfel J, Endres M, Niendorf T, Sobesky J (2012) Ultrahigh-field MRI in human ischemic stroke—a 7 Tesla study. PLoS One 7:e37631. doi:10.1371/journal.pone.0037631
57. Kollia K, Maderwald S, Putzki N, Schlamann M, Theysohn JM, Kraff O, Ladd ME, Forsting M, Wanke I (2009) First clinical study on ultra-high-field MR imaging in patients with multiple sclerosis: comparison of 1.5T and 7T. Am J Neuroradiol 30:699–702. doi:10.3174/ajnr.A1434
58. Lupo JM, Li Y, Hess CP, Nelson SJ (2011) Advances in ultra-high field MRI for the clinical management of patients with brain

tumors. Curr Opin Neurol 24:605–615. doi:10.1097/WCO.0b013e32834cd495
59. Umutlu L, Maderwald S, Kraff O, Kinner S, Schaefer LC, Wrede K, Antoch G, Forsting M, Ladd ME, Lauenstein TC, Quick HH (2012) New look at renal vasculature: 7 Tesla nonenhanced T1-weighted FLASH imaging. J Magn Reson Imaging 36:714–721. doi:10.1002/jmri.23702
60. Suttie JJ, Delabarre L, Pitcher A, van de Moortele PF, Dass S, Snyder CJ, Francis JM, Metzger GJ, Weale P, Ugurbil K, Neubauer S, Robson M, Vaughan T (2012) 7 Tesla (T) human cardiovascular magnetic resonance imaging using FLASH and SSFP to assess cardiac function: validation against 1.5 T and 3 T. NMR Biomed 25:27–34. doi:10.1002/nbm.1708
61. Chang G, Wiggins GC, Xia D, Lattanzi R, Madelin G, Raya JG, Finnerty M, Fujita H, Recht MP, Regatte RR (2012) Comparison of a 28-channel receive array coil and quadrature volume coil for morphologic imaging and T2 mapping of knee cartilage at 7T. J Magn Reson Imaging 35:441–448. doi:10.1002/jmri.23506
62. Umutlu L, Orzada S, Kinner S, Maderwald S, Brote I, Bitz AK, Kraff O, Ladd SC, Antoch G, Ladd ME, Quick HH, Lauenstein TC (2011) Renal imaging at 7 Tesla: preliminary results. Eur Radiol 21:841–849. doi:10.1007/s00330-010-1962-9
63. van de Bank BL, Voogt IJ, Italiaander M, Stehouwer BL, Boer VO, Luijten PR, Klomp DW (2012) Ultra high spatial and temporal resolution breast imaging at 7T. NMR Biomed. doi:10.1002/nbm.2868
64. Cho ZH, Son YD, Kim HK, Kim KN, Oh SH, Han JY, Hong IK, Kim YB (2008) A fusion PET-MRI system with a high-resolution research tomograph-PET and ultra-high field 7.0 T-MRI for the molecular-genetic imaging of the brain. Proteomics 8:1302–1323. doi:10.1002/pmic.200700744
65. Pichler BJ, Judenhofer MS, Catana C, Walton JH, Kneilling M, Nutt RE, Siegel SB, Claussen CD, Cherry SR (2006) Performance test of an LSO-APD detector in a 7-T MRI scanner for simultaneous PET/MRI. J Nucl Med 47:639–647
66. Schlyer D, Vaska P, Tomasi D, Woody C, Maramraju SH, Southekal S et al (2007) A simultaneous PET/MRI scanner based on RatCAP in small animals. In: Proceeding of nuclear science symposium conference record, IEEE, vol 5. doi:10.1109/NSSMIC.2007.4436833
67. Hoge RD, Atkinson J, Gill B, Crelier GR, Marrett S, Pike GB (1999) Linear coupling between cerebral blood flow and oxygen consumption in activated human cortex. Proc Natl Acad Sci USA 96:9403–9408
68. Hyder F, Patel AB, Gjedde A, Rothman DL, Behar KL, Shulman RG (2006) Neuronal-glial glucose oxidation and glutamatergic–GABAergic function. J Cereb Blood Flow Metab 26:865–877. doi:10.1038/sj.jcbfm.9600263
69. Schmidt KC, Turkheimer FE (2002) Kinetic modeling in positron emission tomography. Q J Nucl Med 46:70–85
70. Mangia S, Tkac I, Gruetter R, Van De Moortele PF, Giove F, Maraviglia B, Ugurbil K (2006) Sensitivity of single-voxel ^{1}H-MRS in investigating the metabolism of the activated human visual cortex at 7 T. Magn Reson Imaging 24:343–348. doi:10.1016/j.mri.2005.12.023
71. Oz G, Seaquist ER, Kumar A, Criego AB, Benedict LE, Rao JP, Henry PG, Van De Moortele PF, Gruetter R (2007) Human brain glycogen content and metabolism: implications on its role in brain energy metabolism. Am J Physiol Endocrinol Metab 292:E946–E951. doi:10.1152/ajpendo.00424.2006
72. Catana C, Benner T, van der Kouwe A, Byars L, Hamm M, Chonde DB, Michel CJ, El Fakhri G, Schmand M, Sorensen AG (2011) MRI-assisted PET motion correction for neurologic studies in an integrated MR-PET scanner. J Nucl Med 52:154–161. doi:10.2967/jnumed.110.079343
73. Gutierrez D, Montandon ML, Assal F, Allaoua M, Ratib O, Lovblad KO, Zaidi H (2012) Anatomically guided voxel-based partial volume effect correction in brain PET: impact of MRI segmentation. Comput Med Imaging Graph 36:610–619. doi:10.1016/j.compmedimag.2012.09.001
74. Hinds KA, Hill JM, Shapiro EM, Laukkanen MO, Silva AC, Combs CA, Varney TR, Balaban RS, Koretsky AP, Dunbar CE (2003) Highly efficient endosomal labeling of progenitor and stem cells with large magnetic particles allows magnetic resonance imaging of single cells. Blood 102:867–872. doi:10.1182/blood-2002-12-3669
75. Shapiro EM, Sharer K, Skrtic S, Koretsky AP (2006) In vivo detection of single cells by MRI. Magn Reson Med 55:242–249. doi:10.1002/mrm.20718
76. Sumner JP, Shapiro EM, Maric D, Conroy R, Koretsky AP (2009) In vivo labeling of adult neural progenitors for MRI with micron sized particles of iron oxide: quantification of labeled cell phenotype. Neuroimage 44:671–678. doi:10.1016/j.neuroimage.2008.07.050
77. Lee HY, Li Z, Chen K, Hsu AR, Xu C, Xie J, Sun S, Chen X (2008) PET/MRI dual-modality tumor imaging using arginine–glycine–aspartic (RGD)-conjugated radiolabeled iron oxide nanoparticles. J Nucl Med 49:1371–1379. doi:10.2967/jnumed.108.051243